Mechanism of Direct Coupling between Binding and Induced Structural Change in Regulatory Calcium Binding Proteins†

Stéphane M. Gagné, Monica X. Li, and Brian D. Sykes*

Department of Biochemistry, Medical Research Council Group in Protein Structure and Function, University of Alberta, Edmonton T6G 2H7, Canada

Received December 16, 1996; Revised Manuscript Received February 6, 1997⊗

ABSTRACT: The structural transition in troponin C induced by the binding of two calcium ions involves an "opening" of the structure, an event that triggers skeletal muscle contraction. We have solved the solution structure of a mutant (E41A) of the regulatory domain of skeletal troponin C wherein one bidentate ligand to the calcium in site I is missing. This structure remains "closed" upon calcium binding, indicating that the linkage between calcium binding and the induced conformational change has been broken. This provides a snapshot of skeletal troponin C between the off and on state and thereby valuable insight into the mechanism of regulation within skeletal TnC. Although several factors contribute to the triggering mechanism, the opening of the troponin C structure is ultimately dependent on one amino acid, Glu^{41}. Insights into the structure of cardiac troponin C can also be derived from this skeletal mutant.

Muscle contraction is initiated by the release of Ca^{2+} ions from the sarcoplasmic reticulum triggering a cascade of events involving several protein structural changes and altered protein−protein interactions (Leavis & Gergely, 1984; Zot & Potter, 1987; Ohtsuki et al., 1986; Farah & Reinach, 1995). In vertebrate skeletal and cardiac muscle, the conformational change in TnC[1] resulting from Ca^{2+} binding is the first event in contraction. This response is then passed to other components of the thin filament and ultimately leads to muscle contraction. TnC is a small acidic protein (18 kDa) consisting of two similar globular domains (NTnC and CTnC), each containing two Ca^{2+} binding sites. CTnC contains metal binding sites III and IV (high affinity Ca^{2+}/Mg^{2+} sites), which are always filled in muscle cells, and primarily assumes a structural role. In skeletal muscle, NTnC contains calcium binding sites I and II, which are lower affinity Ca^{2+}-specific sites, and carries out the regulatory function. In cardiac muscle, NTnC binds Ca^{2+} in site II only, as site I is defunct (Tobacman, 1996).

Although the crystal structure of avian skeletal TnC was first solved a decade ago (Herzberg & James, 1988; Satyshur et al., 1988), the structure of the calcium-loaded regulatory domain was first reported last year (Gagné et al., 1995; Slupsky & Sykes, 1995). This provided an experimental structural description of the skeletal muscle contraction switch and confirmed the validity of the proposed model (Herzberg et al., 1986). The structural transition in the regulatory domain of skeletal TnC on Ca^{2+} binding involves an opening of the domain through a large change in interhelical angles (Figure 1). This leads to the increased exposure of an extensive hydrophobic patch (Gagné et al., 1995; Slupsky & Sykes, 1995; Herzberg et al., 1986). Although the structures of the 0Ca-NTnC (Herzberg & James, 1988; Satyshur et al., 1988; Gagné et al., 1995) and 2Ca-NTnC (Gagné et al., 1995; Slupsky & Sykes, 1995; Strynadka et al.[2]) are available, the detailed mechanism of the linkage between Ca^{2+} binding and this Ca^{2+}-induced structural change is still unclear.

We present in this paper the 3D solution structure of a Ca^{2+}-bound mutant of the N-domain of skeletal TnC (2Ca-E41A-NTnC) in which one of the ligands to the Ca^{2+} in site I is missing. This structure is a snapshot of TnC between the off ($-Ca^{2+}$) and on ($+Ca^{2+}$) state and therefore provides valuable insight into the mechanism of regulation within skeletal TnC, that is, the coupling between ligand binding and subsequent structural changes. The results can be applied to other homologous proteins (Ikura, 1996), such as calmodulin (Zhang et al., 1995; Kuboniwa et al., 1995; Finn et al., 1995), in which Ca^{2+} induces conformational changes that modulate their interaction with target proteins. Additionally, insights into the structure of cardiac troponin C can be derived from this skeletal mutant.

The Ca^{2+} binding sites in skeletal TnC involve a pair of HLH in each domain where the Ca^{2+} ions are coordinated. On the basis of crystal structures of HLH Ca^{2+} binding proteins (Strynadka & James, 1989), the six amino acid residues involved in Ca^{2+}-coordination were defined; five are in the loop region (X, Y, Z, −Y, −X positions) and the sixth one (−Z) is in the second helix of the HLH motif. In all regular HLH motifs, the residue at −Z is a glutamate and it contributes both of its side-chain oxygens to the calcium coordination (Strynadka & James, 1989). The

† Supported by MRC Group in Protein Structure and Function. The coordinates for the final structures, along with the set of restraints, have been deposited with the Protein Data Bank (accession code: 1SMG). The coordinates will also be directly accessible on our Web server at http://www.pence.ualberta.ca/~smg3d/e41a.html.

* To whom correspondence should be addressed.

⊗ Abstract published in *Advance ACS Abstracts,* March 15, 1997.

[1] Abbreviations: TnC, troponin C; NTnC, N-terminal domain of TnC; CTnC, C-terminal domain of TnC; 0Ca-NTnC, calcium-free NTnC; 2Ca-NTnC, calcium-bound NTnC; E41A-NTnC, E41A mutant of NTnC; 2Ca-E41A-NTnC, calcium-bound E41A-NTnC; HLH, helix−loop−helix; NMR, nuclear magnetic resonance.

[2] X-ray Crystallographic Analysis of the Calcium-Saturated N-Terminal Domain of Troponin-C at 1.75 Å Resolution, N. C. J. Strynadka, M. Chernaia, A. R. Sielecki, M. X. Li, L. B. Smillie, and M. N. G. James, unpublished data.

S0006-2960(96)03076-0 CCC: $14.00 © 1997 American Chemical Society

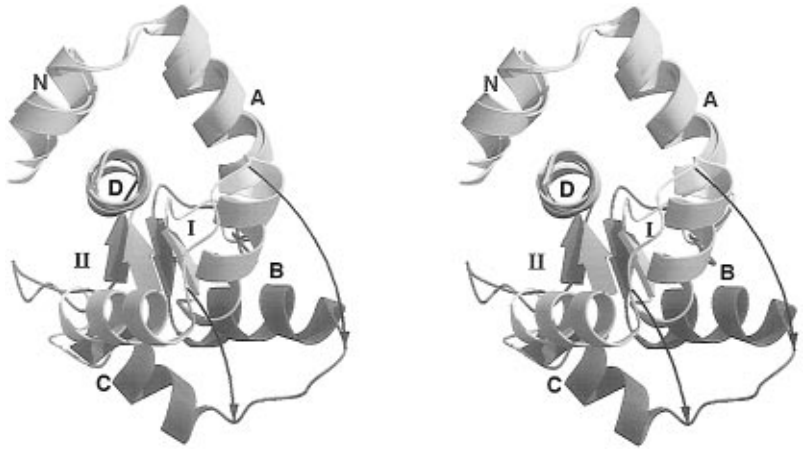

FIGURE 1: Representation of the Ca^{2+}-induced opening of the N-domain of troponin C (Gagné et al., 1995). The apo form (Herzberg & James, 1988) and the $2Ca^{2+}$ form (Gagné et al., 1995) were superimposed using residues in helices N, A, and D (shown in light gray). The movement of the helix B/helix C unit (shown in medium gray for the apo form and in dark gray for the $2Ca^{2+}$ form) upon Ca^{2+} binding is indicated by the arrows. All figures in this paper were produced with the programs Molscript (Kraulis, 1991) and Raster3D (Merritt & Murphy, 1994).

bidentate coordination residue in site I, Glu^{41}, was found to have irregular backbone dihedral angles when NTnC is in the apo form, therefore leading to a "kink" in the B-helix (Herzberg & James, 1988; Satyshur et al., 1988; Gagné et al., 1994, 1995; Strynadka & James, 1989). In the apo form Glu^{41} forms a salt bridge with Lys^{40}, which could potentially contribute to the stabilization of the kink. It was shown that this kink was straightened upon Ca^{2+} binding (Gagné et al., 1994, 1995; Slupsky & Sykes, 1995), and it was postulated that this straightening was critical to the function of the N-domain (Gagné et al., 1994). The behavior of the −Z position in site II is different, and there is no kink in the D-helix of 0Ca-NTnC. It has also been shown that sites I and II have different Ca^{2+} binding affinities (Li et al., 1995) and therefore that Ca^{2+} binding to NTnC was stepwise. Although it was not possible to unambiguously determine the order of binding, it was suggested that site II has the strongest Ca^{2+} affinity (Li et al., 1995).

Our initial goal was to explore the contribution of site I into the calcium induced structural change by making site I defunct. Removal of the bidentate ligand (Glu^{41}) appeared to be the perfect choice since it meant removing two out of seven coordinating oxygens. In addition to the suppression of Ca^{2+} binding to site I, the mutation of Glu^{41} to Ala^{41} was attractive for the following reasons. First, the mutant will be lacking the salt bridge ($Glu^{41}-Lys^{40}$) present in the apo form which potentially stabilizes the kink. Second, alanine is an amino acid having helix propensity. The Glu^{41} to Ala^{41} mutant might therefore have been expected to favor the straightening of the B-helix and the opening of the structure. A "closed" structure of this mutant in the Ca^{2+}-saturated state would therefore have indicated that binding of Ca^{2+} to site I was essential to the structural change.

EXPERIMENTAL PROCEDURES

Cloning, expression, and labeling with either ^{15}N or $^{15}N/^{13}C$ of chicken E41A-NTnC will be described in a future paper.[3] The experimental data were obtained under near-physiological conditions (30 °C, pH 6.7, 100 mM KCl) at a protein concentration of 1.5−2.0 mM and a Ca^{2+} concentration of about 5 equiv. Chemical shift assignments (^1H, ^{15}N, and ^{13}C) were performed using multidimensional heteronuclear NMR experiments acquired on a Unity 600 MHz spectrometer equipped with a triple resonance probe and Z-pulsed field gradient. The following experiments were used for assignments: HNCACB (Muhandiram & Kay, 1994), CBCA(CO)CANNH (Muhandiram & Kay, 1994), 75 and 150 ms ^{15}N-edited-NOESY (Zhang et al., 1994), 57 ms ^{15}N-edited-TOCSY (Zhang et al., 1994), 17 ms HCCH-TOCSY (Kay et al., 1993), 75 and 150 ms ^{13}C-edited-NOESY (Ikura et al., 1990), 2D-COSY in D_2O (Rance et al., 1988), and 150 ms 2D-NOESY (Jeener et al., 1979; Macura & Ernst, 1980) in D_2O. Valine and leucine methyl groups were stereospecifically assigned using a ^{13}C-HSQC of a 30% ^{13}C-labeled sample (Neri et al., 1989). Coupling constants were obtained using an HNHA experiment (Kuboniwa et al., 1994). Spectra were processed using the software package NMRPipe (Delaglio et al., 1995) and analyzed using the program PIPP (Garrett et al., 1991). Interproton distance information was derived from the NOESY experiments listed above. The 2D-NOESY was calibrated on the basis of NOEs corresponding to known distance (Phe $H\delta-H\epsilon = 2.48$ Å). The 75 ms 3D-NOESYs were calibrated using an NOE corresponding to a known distance, located on the same ^{15}N or ^{13}C trace, and an error of 50% was assumed on each NOE intensity. The following distances were used to calibrate the 3D spectra: $HN_i-H\alpha_i = 2.70-3.05$ Å (for residues with negative ϕ), $HN_i-H\alpha_{i-1} = 1.7-3.6$ Å, H−C−C−H = 2.2−3.1 Å, and $H-C-CH_3 = 2.5-2.7$ Å, H−C−H = 1.7−1.8 Å. In cases where direct calibration was not possible, the distance constraints were overestimated. For NOEs found only in the 150 ms NOESYs, the upper bound was set to 6 Å. For all proton-proton restraints, the lower bound was set to 1.7 Å. The Ca^{2+}−ligand distance restraints were set to 2.4 ± 0.4 Å between the Ca^{2+} ion and the oxygens involved in coordinating Ca^{2+} (Strynadka & James, 1989). Dihedral restraints for the ϕ angle were obtained from the HNHA experiment, using a correction factor of 1.055. A 25% error on the peak intensities was assumed, and the minimum ϕ dihedral restraint range was set to ±10°. The initial set of restraints included only a portion of the NOEs found in Table 1, no

[3] M. X. Li, S. M. Gagné, L. Spyracopoulos, C. P. A. M. Kloks, G. Audette, M. Chandra, R. J. Solaro, L. B. Smillie, and B. D. Sykes, unpublished results.

Table 1: Structural Statistics of the 40 Structures of 2Ca-E41A-NTnC [a]

rmsd from exptl distance restraints (Å)	
all (1367)	0.006 ± 0.001
interresidue sequential ($\|i-j\|=1$) (332)	0.006 ± 0.002
interresidue medium range ($1<\|i-j\|\leq 5$) (347)	0.005 ± 0.002
interresidue long range ($\|i-j\|>5$) (209)	0.004 ± 0.001
intraresidue (479)	0.006 ± 0.002
rmsd from exptl dihedral restraints (deg) (72)	0.17 ± 0.05
rmsd from Ca^{2+} coordination restraints (Å) (6)[b]	0.0003 ± 0.0009
rmsd from idealized covalent geometry	
bonds (Å)	0.0012 ± 0.0001
angles (deg)	0.291 ± 0.006
impropers (deg)	0.211 ± 0.004
energies (kcal mol^{-1})	
F_{NOE}[c]	2.2 ± 0.9
F_{cdih}[c]	0.14 ± 0.08
F_{repel}[d]	4.4 ± 1.3
$E_{L\text{-}J}$[e]	−413 ± 30

	backbone atoms	heavy atoms
atomic rmsd (Å)[f]		
residues 1−90	1.08 ± 0.20	1.44 ± 0.14
residues 6−84	0.60 ± 0.11	1.06 ± 0.08
well-defined residues[g]	0.49 ± 0.08	0.88 ± 0.07
helices[h]	0.23 ± 0.07	0.86 ± 0.14
ϕ/ψ in most favored region (%)[i]		91.6
ϕ/ψ in additionally allowed region (%)[i]		8.4

[a] The number of each type of restraints used in the structure calculation is given in parentheses. None of the structures exhibits distance violations greater than 0.24 Å or dihedral violations greater than 1.6°. Standard deviations are given when applicable. [b] The distance restraints to the Ca^{2+} ion in site II were based on the coordination of Ca^{2+} in the crystal structures of TnC and homologous proteins (Strynadka & James, 1989). [c] F_{NOE} and F_{cdih} were calculated using force constants of 50 kcal mol^{-1} and 200 kcal mol^{-1} rad^{-2}, respectively. [d] F_{repel} was calculated using a force constant of 4.0 kcal mol^{-1} $Å^{-4}$ with the van der Waals hard sphere raddi set to 0.75 times those in the parameter set PARALLHSA supplied with X-PLOR (Brünger, 1992). [e] $E_{L\text{-}J}$ is the Lennard-Jones van der Waals energy calculated with the CHARMM empirical energy function (Brünger, 1992) and is not included in the target function for the simulated annealing calculation. [f] Root mean square deviations to the average structure. The average structure was obtained by averaging the coordinates of the individual structures, best fitted to each other, including every residue. [g] Well-defined backbone atoms were found for 67 residues (74%) and included residues 6−29, 36−49, and 56−84. Of the residues having well-defined backbone atoms, 55 residues (82%) had a χ_1 and/or χ_2 circular variance (Laskowski et al., 1993) smaller than 0.4 and were selected as having well-defined side-chain heavy atoms. Those 55 residues are 6−14, 18−20, 22−26, 29, 36, 37, 39, 41−47, 49, 56−66, 68−73, 75−77, and 79−84. [h] Average of the individual helical rms deviations. N(5−13): 0.22 ± 0.07/0.84 ± 0.15 . A(16−28): 0.27 ± 0.07/0.87 ± 0.10. B(42−49): 0.27 ± 0.09/0.82 ± 0.16. C(55−64): 0.22 ± 0.07/1.00 ± 0.17. D(75−84): 0.18 ± 0.05/0.77 ± 0.11. [i] As determined by the program PROCHECK (Laskowski et al., 1993). Only residues 5−84 were considered.

dihedral restraints, and no Ca^{2+} restraints. From this initial set of restraints and starting from an extended structure, 101 structures were generated with the simulated annealing protocol (sa.inp) implemented in X-PLOR (Brünger, 1992), using 12 000 high-temperature steps (60 ps at 1000 K) and 6000 cooling steps (30 ps, final temperature of 100 K). Out of those 101 structures, 50 folded properly (i.e., had significant lower total energy than the rest) and were kept as starting structures for further rounds of refinements. The refinement rounds were also done with the simulated annealing protocol, but using 6000 high-temperature step (30 ps) and 4000 cooling steps (20 ps). The set of structures presented in this paper includes the 40 structures with the lowest total energy selected from the 50 structures obtained in the last round of refinement.

RESULTS

The Ca^{2+} titration of E41A-NTnC revealed an unexpected result; despite removal of the bidentate ligand, site I was still able to bind Ca^{2+} (see Figure S1, Supporting Information). Using an approach similar to the one used in Li et al. (1995), the two dissociation constants were determined to be 10−20 μM and 1−2 mM for site II and site I, respectively.[3] The weak binding was unambiguously assigned to site I, as opposed to nonspecific binding, on the basis of the local chemical shift changes which were observed during the Ca^{2+} titration. The large chemical shift changes which occur between 1 and 5 equiv of Ca^{2+} are localized in site I and are consistent with the ones observed in wild-type NTnC (Gagné et al., 1994). The Ca^{2+} binding constant for site I was reduced by approximately 100-fold relative to wild type (Li et al., 1995), and at the Ca^{2+} concentration used in this study, site I is 80% filled. This brought a completely new focus to the study: monitoring the critical role of a single residue, Glu^{41}, in the function of skeletal troponin C and elucidating the mechanism of the calcium-induced structural change in these proteins.

The 3D structure of 2Ca-E41A-NTnC has been determined using 1439 experimental restraints (Table 1) derived from NMR spectroscopy. Figure 2 shows a stereoview of the best-fit superimposition of the backbone atoms. On the basis of restraint violations, rmsd values, and Ramachandran plots (Table 1), this structure is of high quality. The structure consists of five helices (N, residues 5−13; A, 16−28; B, 42−49; C, 55−64; and D, 75−84) and two calcium-binding loops (I, 30−41, and II, 66−77) connected by a short β-sheet (36−38, 72−74). There is no significant difference in the secondary structure of 2Ca-E41A-NTnC compared with wild-type 0Ca-NTnC and 2Ca-NTnC. The five helices are very well defined, having individual backbone rmsd around 0.23 ± 0.07 Å (Table 1). The β-sheet and site II are also well defined, having backbone rmsd of 0.25 ± 0.08 and 0.24 ± 0.06 Å, respectively. The good definition found in site II is not due to the Ca^{2+} restraints used for the final structure calculation. Structural calculations were made without the Ca^{2+} restraints and yielded a similar definition for site II. Although the Ca^{2+} restraints provide a better definition for the side chains involved in coordination of the ion, the backbone conformation of site II is a result of the experimental NMR data. Unlike site II, site I is not as well defined (backbone rmsd of 0.60 ± 0.22 Å). The poorer definition of site I relative to site II is partially due to the smaller number of experimental restraints. Other poorly defined regions include the N- and C-terminal residues and the B−C linker. Backbone amide ^{15}N relaxation studies[4] have shown that these residues have lower order parameters (S^2), indicating that the poor definition is due at least in part to flexibility and not only to a lack of structural restraints.

Figure 3 compares the average NMR structure of 2Ca-E41A-NTnC with the X-ray structure of 0Ca-NTnC (Herzberg & James, 1988) and the recently solved X-ray structure of 2Ca-NTnC.[2] The quality of the structure presented here is significantly better than the NMR structure of 2Ca-NTnC (Gagné et al., 1995), due to a larger number of medium- and long-range NOEs, to the absence of the dimerization

[4] S. M. Gagné, L. Spyracopoulos, S. Tsuda, L. E. Kay, and B. D. Sykes, unpublished data.

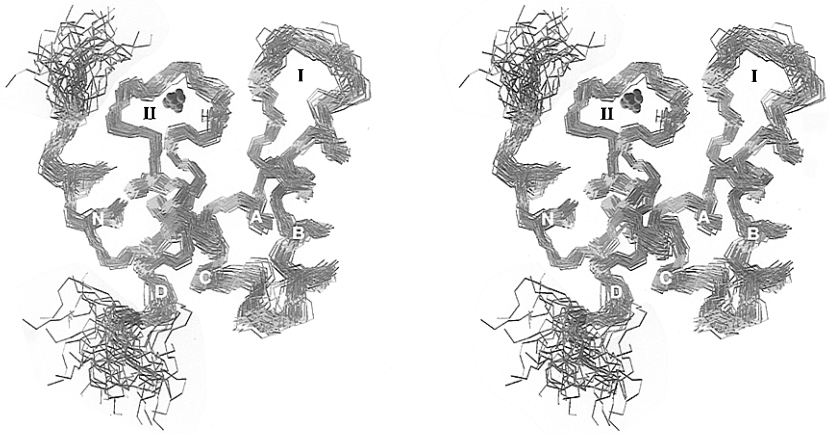

FIGURE 2: Stereoview of the solution structure of 2Ca-E41A-NTnC. The backbone (N, Cα, C′) of the family of 40 structures is shown in "rods" representations, and the site II Ca^{2+} position in each of these structures is shown by a small sphere. Although Ca^{2+} is present in solution in site I, there is no Ca^{2+} shown here because none was used in the calculations, as the coordination state of site I was not known *a priori*. The five helices are labeled N, A, B, C, and D. The two Ca^{2+} binding loops are labeled I and II.

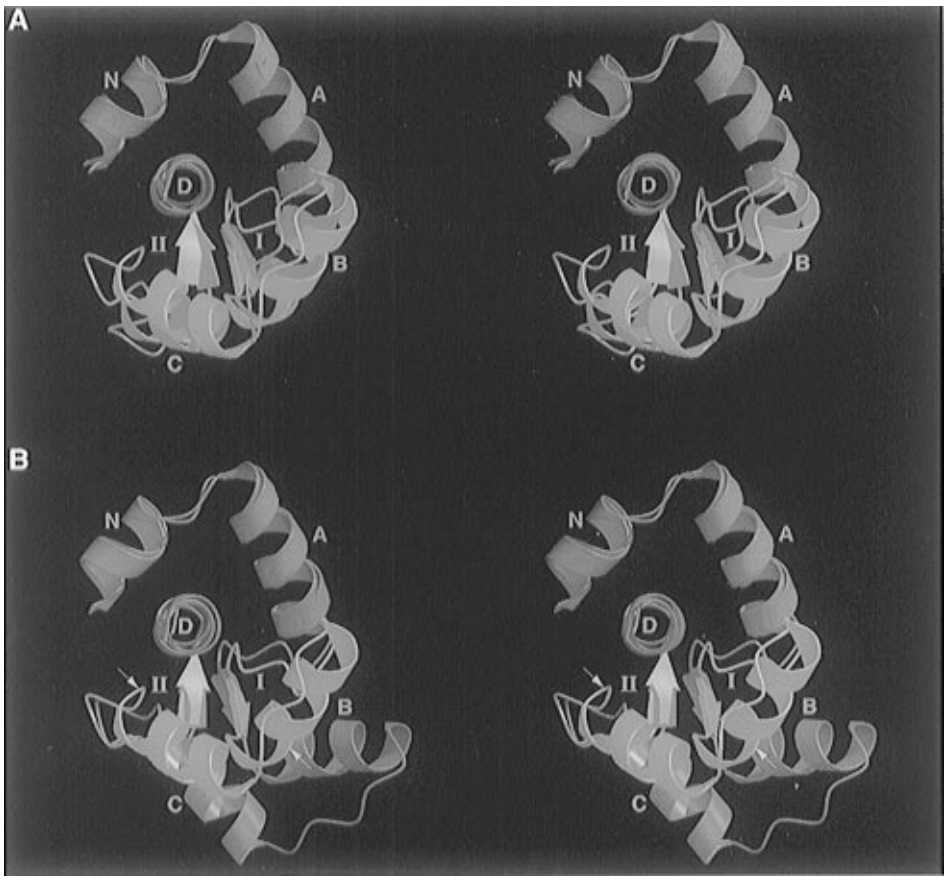

FIGURE 3: (A) Comparison of the 2Ca-E41A-NTnC structure with 0Ca-NTnC (Herzberg & James, 1988). The superimposed region (helices N, A, and D) is shown in red. The helix B/helix C unit is shown in green and cyan for 0Ca-NTnC and 2Ca-E41A-NTnC, respectively. (**B**) Comparison of the 2Ca-E41A-NTnC structure with 2Ca-NTnC.[2] The helix B/helix C unit of 2Ca-NTnC is shown in blue, and the other colours are as in (A). The positions of the two hinges for the opening of the structure (see text) are indicated by arrows.

problem which was present in 2Ca-NTnC (Gagné et al., 1995), and possibly to improvements in the techniques used. We therefore used the recent crystal structure of 2Ca-NTnC as opposed to the NMR structure we previously published (Gagné et al., 1995), since it is of very high resolution (1.78 Å). Comparison of the helix packing in 2Ca-E41A-NTnC with 0Ca-NTnC and 2Ca-NTnC reveals both similarities and differences. The arrangement of helices N, A, and D is virtually identical in all three structures; the backbone rmsd for these residues (5−28, 75−84) with 0Ca-NTnC and 2Ca-NTnC is 0.73 and 0.76 Å, respectively. Since these three helices are not significantly affected by the Ca^{2+} state, this superimposition will be used frequently and will be referred to NAD. The packing of helix B is similar to $0Ca^{2+}$-NTnC (NAD: rmsd of 1.3 Å) and therefore has major differences with 2Ca-NTnC (9.2 Å). Helix C is positioned between 0Ca-NTnC (NAD: rmsd of 2.5 Å) and 2Ca-NTnC (8.8 Å), closer to 0Ca-NTnC. The state of the helix packing of E41A is clearly represented by the measure of its interhelical angles. When compared with the apo or $2Ca^{2+}$ form of TnC and calmodulin, the interhelical angles of 2Ca-E41A-NTnC are like the apo forms, rather than the $2Ca^{2+}$ forms (Table 2). We have also looked at the accessible surface area of the nonpolar groups, which is a measure of the exposure of the

Table 2: Interhelical Angles in Troponin C and Calmodulin as a Function of Ca^{2+}

protein	interhelical angle (deg)[a]	
	first site[b]	second site[b]
average of apo forms[c]	135 ± 5	134 ± 9
average of $2Ca^{2+}$ forms[d]	95 ± 9	91 ± 11
Ca^{2+}-E41A-NTnC[e]	130 ± 3	130 ± 5

[a] The axis orientation for an α-helix was defined by two points, where the first point is the average of the first 11 backbone atoms and the second point is the average of the last 11 backbone atoms. [b] First site corresponds to the A−B helix pair for N-domains and to the E−F helix pair for C-domains. Similarly, second site corresponds to the C−D and G−H helix pair for N-domains and C-domains, respectively. [c] Average of nine apo domains found in the PDB data bank. PDB accession codes: 1TNP, 5TNC, 4TNC, 1TOP, 1DMO, 1CFC, and 1CMF. [d] Average of 27 Ca^{2+}-saturated domains found in the PDB data bank. PDB accession codes: 1TNQ, 1TNW, 1OSA, 1CLL, 3CLN, 4CLN, 1LIN, 1CTR, 1CDM, 1CDL, 2BBN, 5TNC, 4TNC, 1TOP, 1PON, 1CMG, and 2Ca-NTnC[2]. [e] Present study.

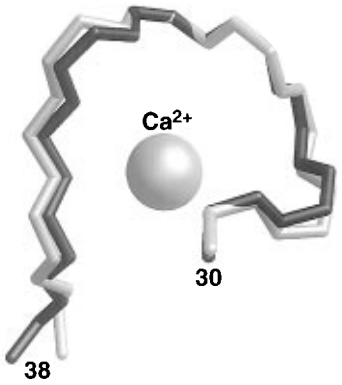

FIGURE 4: Superimposition of site I (residues 30−38) in 2Ca-NTnC[2] (light gray) and 2Ca-E41A-NTnC (dark gray). The good overlap indicates that the mutational change did not affect the way calcium sits in the binding pocket. Note that the Ca^{2+} ion was not included in site I for the structure calculations.

hydrophobic patch. Using the Shrake definitions (Shrake & Rupley, 1973) and considering only residues 4−88, the following values were observed: 2872 ± 74 Å^2 for 2Ca-E41A-NTnC, 2866 Å^2 for 0Ca-NTnC, and 3386 Å^2 for 2Ca-NTnC. These values show that the hydrophobic patch is not exposed in 2Ca-E41A-NTnC.

As expected, site II adopts a conformation very close to the 2Ca-NTnC one (NAD: rmsd of 0.99 Å). When site II is superimposed (residues 66−77), the Ca^{2+} position in 2Ca-E41A-NTnC is only 0.26 Å away from the one in 2Ca-NTnC. Similarly, site I has a conformation similar to the 2Ca-NTnC one as far as residues 30−38 are concerned (Figure 4). As was pointed out previously (Service, 1995), it is important that the mutation does not change the way Ca^{2+} sits in the binding pocket.

DISCUSSION

Muscle contraction is triggered by the Ca^{2+}-induced conformational change that occurs in the regulatory domain of TnC. Upon binding of two Ca^{2+} ions, the N-domain of TnC "opens" and exposes a large hydrophobic patch (Gagné et al., 1995; Slupsky & Sykes, 1995; Herzberg et al., 1986). A similar structural change occurs in calmodulin upon Ca^{2+} binding (Zhang et al., 1995; Kuboniwa et al., 1995; Finn et al., 1995). Although the Ca^{2+}-induced structural change found in these proteins is now well determined (Gagné et al., 1995; Slupsky & Sykes, 1995; Zhang et al., 1995; Kuboniwa et al., 1995; Finn et al., 1995), the mechanism by which Ca^{2+} causes the "opening" in not known. The structure of 2Ca-E41A-NTnC provides a unique tool to understand how proteins like TnC and calmodulin operate, as it is a snapshot of NTnC just prior to the opening. As shown above, binding of Ca^{2+} to site II does not trigger the opening of the N-domain. Only minor structural changes occur upon Ca^{2+} binding in E41A-NTnC. Binding of Ca^{2+} to site II, which has been shown to be important (Sheng et al., 1990; Sorenson et al., 1995), requires rearrangement of the ligands and the loop which can be accommodated without opening the domain. Similarly, binding of Ca^{2+} to site I (Glu^{41} not coordinated) does not open the N-domain. This demonstrates that the ligands in site I, with the exception of Glu^{41}, can coordinate Ca^{2+} with only minor rearrangements, as was originally proposed (Strynadka & James, 1989). Exposure of the hydrophobic patch is an unfavorable event, and therefore the opening will not occur unless it is necessary and energetically favorable. As shown in Figure 5, the two oxygens of Glu^{41} in 0Ca-NTnC are 10.8 Å away from the Ca^{2+} position. These oxygens must approach the Ca^{2+} ion to 2.4 Å (Strynadka & James, 1989) in order for site I to bind Ca^{2+} properly. Unlike the other ligands in site I and II, Glu^{41} cannot coordinate the Ca^{2+} ion when the domain is in the closed form. To reach the Ca^{2+}, Glu^{41} causes changes in the backbone dihedral angle at the base of helix B, which result in a reorientation of the helix B/helix C unit. We therefore conclude that it is the coordination of Glu^{41} to the Ca^{2+} ion that ultimately leads to the opening of the domain and that the other ligands play a role in positioning the Ca^{2+} and setting the stage for Glu^{41}. Glu^{41} literally "locks" the domain in the open form.

The two hinges in this structural reorientation occur at the beginning of helix B (primarily at residue Glu^{41}) and at the end of helix C (primarily at residue Val^{65}) (indicated by arrows in Figure 3B). The identification of Val^{65} as the hinge at the C-terminal end of the helix B/helix C unit is based on the observation that the backbone change that occurs at Val^{65} when NTnC binds two Ca^{2+} is not found in 2Ca-E41A-NTnC (Table 3). The backbone dihedral angles of Val^{65} in 2Ca-E41A-NTnC are identical, within experimental errors, to the one of 0Ca-NTnC (Table 3). The best experimental measure of the ϕ dihedral angle in solution is the backbone coupling constant, $^3J_{HN-H\alpha}$. The coupling constant measured for Val^{65} in 2Ca-E41A-NTnC (7.5 Hz) is similar to the one observed in the NMR data of 0Ca-NTnC (7.4Hz; Gagné et al., 1994) and to the one expected from the crytal structure of 0Ca-NTnC (−84° ⇒ 7.3 Hz) but significantly different from the one expected for the crystal structure of 2Ca-NTnC (−115° ⇒ 9.8 Hz) (the $^3J_{HN-H\alpha}$ was not obtained in the NMR data of 2Ca-NTnC; Gagné et al., 1994). It is interesting to note that the dihedral changes that occur at the two hinges are similar, but opposite in direction (Table 3).

To investigate the mechanism further, we have done the following experiment. We looked at an E77A mutant of NTnC,[5] Glu^{77} being the site II homologue of Glu^{41}. Preliminary results showed that this mutant was unable to bind any Ca^{2+} strongly. Similar Ca^{2+} binding properties were observed for comparable mutants (Glu → Gln) of calmodulin (Maune et al., 1992). This inability of site I to bind Ca^{2+}

[5] S. M. Gagné, J. Pearlstone, and B. D. Sykes, unpublished data.

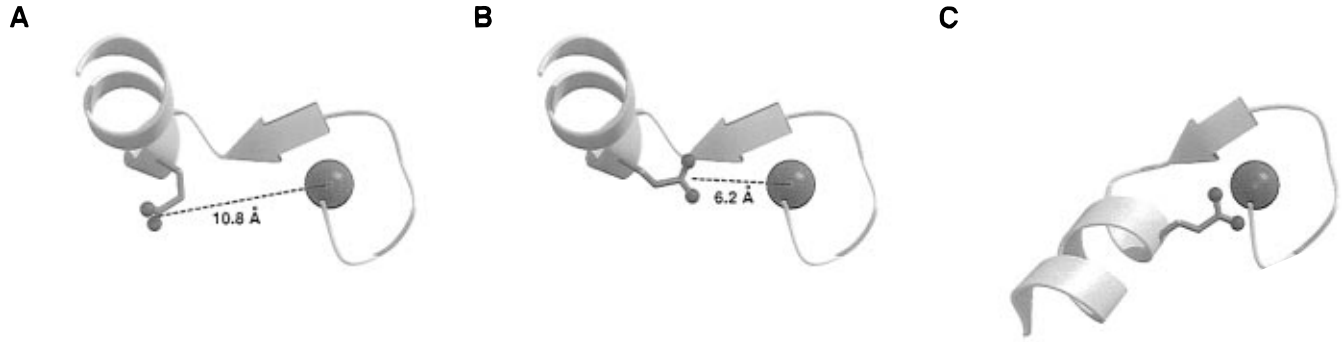

FIGURE 5: Glu^{41} cannot coordinate the Ca^{2+} ion when the domain is in the closed form. The backbone of loop I and helix B are shown in light gray, the side chain of Glu^{41} is shown in the dark gray stick representation, the position of the Ca^{2+} ion is shown by the large sphere, and the coordination oxygens of Glu^{41} are shown by small spheres. The indicated distance is between the Ca^{2+} ion and the centre of the two coordinating oxygens. (A) Glu^{41} in closed form (0Ca-NTnC) (Herzberg & James, 1988). The kink at residue Glu^{41} is clearly visible. (B) Same as in (A) but with the side-chain χ_1 and χ_2 angles of Glu^{41} modified in order to minimize the distance of the ligands to the Ca^{2+} ion. The coordinating oxygens are still 6.2 Å away the Ca^{2+} ion, 3.8 Å short of the coordinating distance (2.4 Å; Strynadka & James, 1989). (C) Glu^{41} in 2Ca-NTnC.[2]

Table 3: Backbone Dihedral Angle at the Hinge Positions as a Function of Ca^{2+}

dihedral angle	0Ca-NTnC[a]	2Ca-NTnC (X-ray)[2]	2Ca-NTnC (NMR)[b]	2Ca-E41A-NTnC
Glu^{41}, ϕ	−96	−65	−66 ± 10	−83 ± 7
Glu^{41}, ψ	−7	−43	−47 ± 9	−13 ± 8
Val^{65}, ϕ	−84	−115	N/A[c]	−89 ± 7
Val^{65}, ψ	−37	−1	N/A[c]	−34 ± 8

[a] PDB accession code 5TNC. [b] PDB accession code 1TNQ. [c] The backbone dihedral angles of Val^{65} are not defined in the NMR structure, due to a lack of restraints.

strongly when site II is perturbed shows that although complete Ca^{2+} binding to site I causes the opening, calcium binding to site II is first required. We previously determined the two different Ca^{2+} binding constants of the N-domain (Li et al., 1995), but we were unable to unambiguously associate them to their corresponding sites. The results presented here clearly indicate that the strongest Ca^{2+} binding occurs in site II. The Ca^{2+} binding scenario for NTnC is therefore the following: the first Ca^{2+} binds to site II, causing only minor conformational changes but setting the stage; then the second Ca^{2+} binds to site I, causing the structural change required to trigger skeletal muscle contraction.

As mentioned earlier, the structure of this skeletal mutant can potentially be used as a model for cardiac TnC which is unable to bind Ca^{2+} in site I. Cardiac TnC is 70% homologous to skeletal TnC, and the majority of the differences occur in the first 40 residues. The results presented here strongly suggest that the Ca^{2+}-induced structural change in cardiac TnC does not involve an extensive opening of the structure as was found for skeletal TnC, as there is no calcium in site I. Since cardiac and skeletal TnC are nearly identical in the second HLH (site II), it is very likely that the Ca^{2+}-saturated structure of cardiac NTnC resemble 2Ca-E41A-NTnC more than 2Ca-NTnC. This has recently been verified with the determination of the Ca^{2+}-bound cardiac TnC structure.[6]

The mechanism of the direct coupling between calcium binding and induced structural change can be summarized as follows. First, the opening of the structure exposes a large hydrophobic patch, an event which is energetically unfavorable in water ($\Delta G \approx 2.0$ kcal mol^{-1}; Foguel et al., 1996). This exposure can only occur if the favorable interactions associated with Ca^{2+} binding compensate for it and if the binding of Ca^{2+} cannot be accommodated in the closed form. Second, the structural change is defined as a hinge motion between two units, one including the N, A, and D helices and the other the B and C helices. Finally, the movement of the BC unit relative to the NAD unit, which involves the diplacement of several residues by more than 15 Å, is driven by a single amino acid, Glu^{41}.

Clearly, several factors contribute to the regulation of muscle contraction. However, we have shown that the "muscular work" (i.e., opening of the regulatory domain of skeletal TnC to trigger contraction) was accomplished by Glu^{41} reaching for the Ca^{2+} ion, and one could look at it as "flexing muscle with one amino acid" (Service, 1995).

[6] S. K. Sia, M. X. Li, L. Spyracopoulos, S. M. Gagné, W. Liu, J. A. Putkey, and B. D. Sykes, unpublished data.

ACKNOWLEDGMENT

We thank D. Corson, L. Golden, M. Chandra, and L. B. Smillie for assistance with the E41A-NTnC sample preparation; J. Pearlstone for the E77A-NTnC sample preparation; L. E. Kay for providing the pulse sequences essential to this project; G. McQuaid for keeping the spectrometer at optimum performance; J. L. Willard, T. Jellard, and R. Boyko (Mission Control) for computer expertise; N. C. J. Strynadka and M. N. G. James for supplying us with the coordinates of 2Ca-NTnC prior to publication and public release and for critical reading of the manuscript; R. McKay and L. Spyracopoulos for critical reading of the manuscript; and the Protein Engineering Network Centre of Excellence (PENCE) for the use of their Unity 600 NMR spectrometer.

SUPPORTING INFORMATION AVAILABLE

A binding curve showing Ca^{2+} binding to site I (Figure S1), a labeled 2D-^{15}N-HSQC (Figure S2), the methyl region of a 2D-^{13}C-CT-HSQC (Figure S3), and a strip plot of the 150 ms 3D-^{15}N-edited-NOESY (Figures S4−A,B) (5 pages). Ordering information is given on any current masthead page.

REFERENCES

Brünger, A. T. (1992) *X-PLOR Version 3.1. A System for X-ray Crystallography and NMR*, Yale University Press, New Haven, CT.

Delaglio, F., Grzesiek, S., Vuister, G. W., Zhu, G., Pfeifer, J., & Bax, A. (1995) *J. Biomol. NMR 6*, 277.

Farah, C. S., & Reinach, F. C. (1995) *FASEB J. 9*, 755.
Finn, B. E., Evenäs, J., Drakenberg, T., Waltho, J. P., Thulin, E., & Forsén, S. (1995) *Nat. Struct. Biol. 2*, 777.
Foguel, D., Suarez, M. C., Barbosa, C., Rodrigues, J. J., Sorenson, M. M., Smillie, L. B., & Silva, J. L. (1996) *Proc. Natl. Acad. Sci. U.S.A. 93*, 10642.
Gagné, S. M., Tsuda, S., Li, M. X., Chandra, M., Smille, L. B., & Sykes, B. D. (1994) *Protein Sci. 3*, 1961.
Gagné, S. M., Tsuda, S., Li, M. X., Smillie L. B., & Sykes, B. D (1995) *Nat. Struct. Biol. 2*, 784.
Garrett, D. S., Powers, R., Gronenborn, A. M., & Clore, G. M (1991) *J. Magn. Reson. 95*, 214.
Herzberg, O., & James, M. N. G. (1988) *J. Mol. Biol. 203*, 761.
Herzberg, O., Moult, J., & James, M. N. G. (1986) *J. Biol. Chem. 261*, 2638.
Ikura, M. (1996) *Trends Biochem. Sci. 21*, 14.
Ikura, M., Kay, L. E., Tschudin, R., & Bax, A. (1990) *J. Magn. Reson. 86*, 204.
Jeener, J., Meier, B. H., Bachmann, P., & Ernst, R. R. (1979) *J. Chem. Phys. 71*, 4546.
Kay, L. E., Xu, G. Y., Singer, A. U., Muhandiram, D. R., & Forman-Kay, J. D. (1993) *J. Magn. Reson. B 101*, 333.
Kraulis, P. J. (1991) *J. Appl. Crystallogr. 24*, 946.
Kuboniwa, H., Grzesiek, S., Delaglio, F., & Bax, A. (1994) *J. Biomol. NMR 4*, 871.
Kuboniwa, H., Tjandra, N., Grzesiek, S., Ren, H., Klee, C. B., & Bax, A. (1995) *Nat. Struct. Biol. 2*, 768.
Laskowski, R. A., MacArthur, M. W., Moss, D. S., & Thornton., J. M. (1993) *J. Appl. Crystallogr. 26*, 283.
Leavis, P. C., & Gergely, J. (1984) *CRC Crit. Rev. Biochem. 16*, 235.
Li, M. X., Gagné, S. M., Tsuda, S., Kay, C. M., Smillie, L. B., & Sykes, B. D. (1995) *Biochemistry 34*, 8330.
Macura, S., & Ernst, R. R. (1980) *Mol. Phys. 41*, 95.
Maune, J. F., Klee, C. B., & Beckingham, K. (1992) *J. Biol. Chem. 267*, 5286.
Merritt, E. A., & Murphy, E. P. M. (1994) *Acta Crystallogr. D50*, 869.
Muhandiram, D. R., & Kay, L. E. (1994) *J. Magn. Reson. B 103*, 203.
Neri, D., Szyperski, T., Otting, G., Senn, H., & Wüthrich, K. (1989) *Biochemistry 28*, 7510.
Ohtsuki, I., Maruyama, K., & Ebashi, S. (1986) *Adv. Protein Chem. 38*, 1.
Rance, M., Søcrensen, O. W., Bodenhaussen, G., Wagner, G., & Ernst, R. R. (1988) *Biochem. Biophys. Res. Commun. 117*, 479.
Satyshur, K. A., Rao, S. T., Pyzalska, D., Drendel, W., Greaser, M., & Sundaralingam, M. (1988) *J. Biol. Chem. 263*, 1628.
Service, R. F. (1995) *Science 271*, 31.
Sheng, Z., Strauss, W. L., Francois, J. M., & Potter, J. D. (1990) *J. Biol. Chem. 265*, 21554.
Shrake, A., & Rupley, J. A. (1973) *J. Mol. Biol. 79*, 351.
Slupsky, C. M., & Sykes, B. D. (1995) *Biochemistry 34*, 15953.
Sorenson, M. M., da Silva, A. C., Gouveia, C. S., Sousa, V. P., Oshima, W., Ferro, J. A., & Reinach, F. C. (1995) *J. Biol. Chem. 270*, 9770.
Strynadka, N. C. J., & James, M. N. G. (1989) *Annu. Rev. Biochem. 58*, 951.
Tobacman, L. S. (1996) *Annu. Rev. Physiol. 58*, 447.
Zhang, M., Tanaka, T., & Ikura, M. (1995) *Nat. Struct. Biol. 2*, 758.
Zhang, O., Kay, L. E., Olivier, J. P., & Forman-Kay, J. D. (1994) *J. Biomol. NMR 4*, 845.
Zot, A. S., & Potter, J. D. (1987) *A. Rev. Biophys. Biophys. Chem. 16*, 535.

BI963076+